

## Improved ferroelectric and piezoelectric properties of $(\text{Na}_{0.5}\text{K}_{0.5})\text{NbO}_3$ ceramics via sintering in low oxygen partial pressure atmosphere and adding LiF

Bing-Yu Li\*, Xiao-Ming Chen\*<sup>‡</sup>, Mei-Dan Liu\*, Zi-De Yu\*,  
Han-Li Lian<sup>†</sup> and Jian-Ping Zhou\*

\*School of Physics and Information Technology  
Shaanxi Normal University  
Xi'an 710119, P. R. China

<sup>†</sup>School of Science  
Xi'an University of Posts and Telecommunications  
Xi'an 710121, P. R. China

<sup>‡</sup>xmchen@snnu.edu.cn

Received 19 February 2021; Revised 21 March 2021; Accepted 2 April 2021; Published 23 April 2021

Dense  $(\text{Na}_{0.5}\text{K}_{0.5})\text{NbO}_3$  lead-free ceramics with the simple composition were prepared via sintering in low oxygen partial pressure ( $\text{pO}_2$ ,  $\sim 10^{-12}$  atm) atmosphere and adding LiF. All the ceramics have pure orthorhombic structure. Compared to the LiF-added  $(\text{Na}_{0.5}\text{K}_{0.5})\text{NbO}_3$  ceramics sintered in air and the low  $\text{pO}_2$ -sintered pure  $(\text{Na}_{0.5}\text{K}_{0.5})\text{NbO}_3$  ceramics without LiF addition, the present ceramics exhibit improved piezoelectric and ferroelectric properties. The piezoelectric constant  $d_{33}$  is 125 pC/N, and the converse piezoelectric constant  $d_{33}^*$  is 186 pm/V. The dielectric constant and dielectric loss of the ceramics at room temperature and 1 kHz are 451 and 0.03, respectively. Under the measured electric field of 70 kV/cm, the remanent polarization is 25.9  $\mu\text{C}/\text{cm}^2$  and the coercive field is 13.9 kV/cm. Furthermore, if the base metals such as Cu and Ni powders were mixed into the green pellets and sintered in the low  $\text{pO}_2$  atmosphere, the base metals cannot be oxidized, suggesting possibility of using base metals as electrodes.

**Keywords:** Ceramics; dielectric properties; ferroelectric properties; piezoelectric properties;  $\text{Na}_{0.5}\text{K}_{0.5}\text{NbO}_3$ .

### 1. Introduction

Sodium potassium niobate (KNN)-based lead-free ceramics have been extensively studied. The KNN ceramics with simple compositions always exhibit poor piezoelectric and ferroelectric properties. By co-doping various elements, the piezoelectric properties of KNN-based ceramics can be improved at the cost of complicated compositions. An ultrahigh  $d_{33}$  of  $650 \pm 20$  pC/N has been reported in the system  $(0.96-x)\text{K}_{0.48}\text{Na}_{0.52}\text{Nb}_{0.95}\text{Sb}_{0.05}\text{O}_3-0.04\text{Bi}_{0.5}(\text{Na}_{0.82}\text{K}_{0.18})_{0.5}\text{ZrO}_3-0.4\%\text{Fe}_2\text{O}_3-x\text{AgSbO}_3$  via the multiphase coexistence, which needs nine kinds of elements at least.<sup>1</sup> Wu *et al.* reported that the ceramics  $(1-x)\text{K}_{0.5}\text{Na}_{0.5}\text{Nb}_{0.96}\text{Sb}_{0.04}\text{O}_3-x\text{Bi}_{0.5}\text{Na}_{0.5}\text{Zr}_{0.8}\text{Sn}_{0.2}\text{O}_3$  exhibited good temperature stability of piezoelectric constant, in which an orthorhombic-tetragonal phase boundary can be obtained by using eight kinds of elements.<sup>2</sup> By adding  $\text{BiFeO}_3$ , the phase transition temperatures of  $(1-x)\text{K}_{0.4}\text{Na}_{0.6}\text{NbO}_3-x\text{BiFeO}_3$  were adjusted, which shows good temperature stability.<sup>3</sup> In  $(1-x)(\text{K}_{1-y}\text{Na}_y)\text{NbO}_3-x(\text{Bi}_{1/2}\text{Na}_{1/2})\text{ZrO}_3$  lead-free piezoelectric ceramics, the increase of the  $(\text{Bi}_{1/2}\text{Na}_{1/2})\text{ZrO}_3$  concentration and the adjustment of the  $\text{Na}^+$  ratio can affect morphotropic phase boundary and improve electrical properties.<sup>4</sup> The more complex the composition is, the more

difficult it is in precisely controlling composition for volume production. In addition, there are still some other problems for KNN-based ceramics, such as volatilization of alkali elements during high-temperature sintering process, co-firing base metal electrodes, etc. For overcoming these problems, various methods have been used. Excessive  $\text{K}^+$  and  $\text{Na}^+$  can compensate for the loss of element volatilization during high-temperature sintering process and improve piezoelectric properties of the ceramics.<sup>5</sup> Sintering aids<sup>6-9</sup> and special sintering techniques including spark plasma sintering,<sup>10</sup> two-step sintering,<sup>11</sup> hot-press sintering,<sup>12,13</sup> and sintering in different atmospheres<sup>14-19</sup> can also improve densification and electrical properties of KNN-based ceramics. Reimann *et al.* studied the effect of low oxygen partial pressure ( $\text{pO}_2$ ) sintering and reoxidation annealing on phase structure and electrical properties of Li- and Ta- modified KNN-based ceramics and found that the  $\text{pO}_2$  values during reoxidation process can change phase composition.<sup>14</sup> Fisher *et al.* found that grain sizes of  $(\text{Na}_{0.5}\text{K}_{0.5})\text{NbO}_3$  ceramics are closely related to sintering atmospheres.<sup>16</sup> Kobayashi *et al.* reported that reducing atmosphere-fired KNN-based ceramics had higher resistivity compared to those fired in air atmosphere.<sup>17</sup> Cen *et al.* found that

<sup>‡</sup>Corresponding author.

the valence of Mn ions was more stable in the MnO-doped  $0.955\text{K}_{0.5}\text{Na}_{0.5}\text{NbO}_3\text{-}0.045\text{Bi}_{0.5}\text{Na}_{0.5}\text{ZrO}_3$  ceramics sintered in a reducing atmosphere, and the ceramics exhibited higher fraction of rhombohedral phase compared to those sintered in air.<sup>18</sup>

In our previous work, we have reported a homebuilt low partial pressure ( $\text{pO}_2$ ) firing system and that the pure  $\text{K}_{0.5}\text{Na}_{0.5}\text{NbO}_3$  ceramics were sintered in the system.<sup>19</sup> Compared to the  $\text{Na}_{0.5}\text{K}_{0.5}\text{NbO}_3$  ceramics sintered in air, the low  $\text{pO}_2$  sintered  $\text{K}_{0.5}\text{Na}_{0.5}\text{NbO}_3$  ceramics exhibited higher densification and better electrical properties.<sup>19</sup> Low  $\text{pO}_2$  sintering can significantly suppress volatilization of alkali elements during high-temperature sintering process, thereby reducing point defects in the ceramics. Furthermore, low  $\text{pO}_2$  sintering atmosphere could be useful in co-firing with base metal electrodes including Ni and Cu.

As is well known, LiF is one of the sintering aids with the melting point of  $845^\circ\text{C}$ . The adding of LiF into the ceramics facilitates promoting compaction.<sup>20</sup> Furthermore, the radius of  $\text{F}^-$  ( $1.33 \text{ \AA}$ ) is similar with that of  $\text{O}^{2-}$  ( $1.40 \text{ \AA}$ ) in the case of coordination number 6.<sup>21</sup> The substitution of  $\text{F}^-$  for  $\text{O}^{2-}$  can further decrease oxygen vacancy concentration. Therefore, it is expected that piezoelectric and ferroelectric properties of KNN-based ceramics can be improved via sintering in low  $\text{pO}_2$  atmosphere and adding LiF.

In this study, dense  $(\text{Na}_{0.5}\text{K}_{0.5})\text{NbO}_3$  lead-free ceramics were prepared via sintering in low  $\text{pO}_2$  atmosphere and adding LiF. Their microstructure, ferroelectric, and piezoelectric properties were studied in detail. The electrical properties of the present ceramics were also compared with those of the ceramics with the same composition sintered in air and the pure  $\text{K}_{0.5}\text{Na}_{0.5}\text{NbO}_3$  ceramics without LiF sintered in low  $\text{pO}_2$  atmosphere.

## 2. Experimental Procedures

The LiF-added  $\text{K}_{0.5}\text{Na}_{0.5}\text{NbO}_3$  (denoted as KNN-LiF for convenience) ceramics were prepared. The raw powders are  $\text{K}_2\text{CO}_3$  (99.0%),  $\text{Na}_2\text{CO}_3$  (99.8%),  $\text{Nb}_2\text{O}_5$  (99.5%), and LiF (99.0%) (Sinopharm Chemical Reagent Co., Ltd., Shanghai, China), which were dried at  $120^\circ\text{C}$  for 24 h. The powders were weighed according to the composition of  $(\text{Na}_{0.5}\text{K}_{0.5})\text{NbO}_3$ . The mixture was ball milled for 24 h in ethanol. Then, the powders were calcined at  $850^\circ\text{C}$  for 2 h. Both the heating and cooling rates are  $180^\circ\text{C/h}$ . The 2 mol% LiF was added into the calcined powders and milled again for 12 h. Then, the green pellets were cold isostatic pressed at 200 MPa. The diameter and thickness of the pellets are around 10 mm and 1 mm, respectively. The pellets were sintered at  $1065^\circ\text{C}$  for 3 h in the homebuilt low  $\text{pO}_2$  firing system with  $\text{pO}_2 \sim 10^{-12}$  atm. The  $\text{pO}_2$  is controlled by adjusting the flow rates of the mixed gas including dry nitrogen, saturated wet nitrogen (water vapor and nitrogen), and hydrogen, which has been introduced in our previous work.<sup>19</sup> The flow rates of dry nitrogen, wet nitrogen, and hydrogen are 464 cc/min, 20 cc/

min, and 16 cc/min, respectively. For comparison, the ceramics with the same composition were also sintered in air using the same synthesis parameters.

Microstructure was observed via a scanning electron microscope (SEM, NovaNano450) with an energy dispersive spectrometer (EDS, Bruker Quantax 200). Crystallite structure was detected by using X-ray diffraction (XRD, Rigaku D/Max 2550) with  $\text{Cu K}\alpha$  radiation. The crystallite structure was refined via the General Structure Analysis System (GSAS) software package.<sup>22,23</sup> Archimedes method was used to measure bulk densities of the ceramics. In order to measure piezoelectric constant  $d_{33}$ , the ceramics were poled at 40 kV/cm in silicone oil for 15 min at room temperature and then placed for 24 h.  $d_{33}$  was measured via a quasi-static  $d_{33}$  meter (ZJ-4A). Dielectric properties were measured with an Agilent E4980A LCR meter. Ferroelectric properties were measured using a ferroelectric analyzer (Precision Premier II).

## 3. Results and Discussion

A typical SEM image of the fractured surface of the low  $\text{pO}_2$  fired KNN-LiF ceramic is shown in Fig. 1(a). The ceramics show dense microstructure. The grains exhibit square shape and the mean size is approximate  $2 \mu\text{m}$ . The corresponding compositional maps via EDS analysis are shown in Fig. 1(b). It is found that the elements Na, K, Nb, and F are uniformly distributed inside the grains. No aggregation of the elements was observed. Due to the X-ray absorption characteristic of element Li in the detector window, element Li cannot be detected, as reported by others.<sup>24</sup> Figure 1(c) shows the XRD curve of the ceramic. The sample exhibits pure orthorhombic phase without detectable secondary phase. The diffraction peaks can be well indexed according to the JCPDS No. 71-0946.<sup>25</sup> The crystallite structure was refined [Fig. 1(d)]. The residual factor of the structural refinement is less than 12%. The lattice parameters are  $a = 3.95(0) \text{ \AA}$ ,  $b = 5.68(3) \text{ \AA}$ ,  $c = 5.66(1) \text{ \AA}$ , and lattice volume ( $V$ ) is  $127.0(1) \text{ \AA}^3$ . The theoretical density ( $\rho_t$ ) was calculated via the following formula:  $\rho_t = \text{MZ}/(V \times 6.02 \times 10^{23})$ , where  $M$  is molar mass, and  $Z$  is number of subcell. The obtained  $\rho_t$  is  $4.51 \text{ g/cm}^3$ . The bulk densities ( $\rho_b$ ) of the ceramics fired in the low  $\text{pO}_2$  atmosphere were measured to be  $4.35 \text{ g/cm}^3$ . The relative density can be obtained via  $\rho_r = \rho_b/\rho_t$ , which is 96% and higher than that of the ceramic with the same composition sintered in air ( $\sim 92\%$ ). Via firing in the low  $\text{pO}_2$  atmosphere and adding LiF, the dense ceramics with high relative density were obtained.

The polarization-electric field ( $P$ - $E$ ) loops of the low  $\text{pO}_2$  fired KNN-LiF ceramic measured at 1 Hz and room temperature are shown in Fig. 2(a). The amplitude of the measurement electric fields was increased from 5 kV/cm to 70 kV/cm. With the increase of amplitude of the measurement electric field, the  $P$ - $E$  loops exhibit typical ferroelectric hysteresis character and tend to be saturated. The values of coercive field  $E_c$ , remnant polarization  $P_r$ , and maximum polarization  $P_m$  were obtained via the  $P$ - $E$  loops and are shown in Fig. 2(b). As the

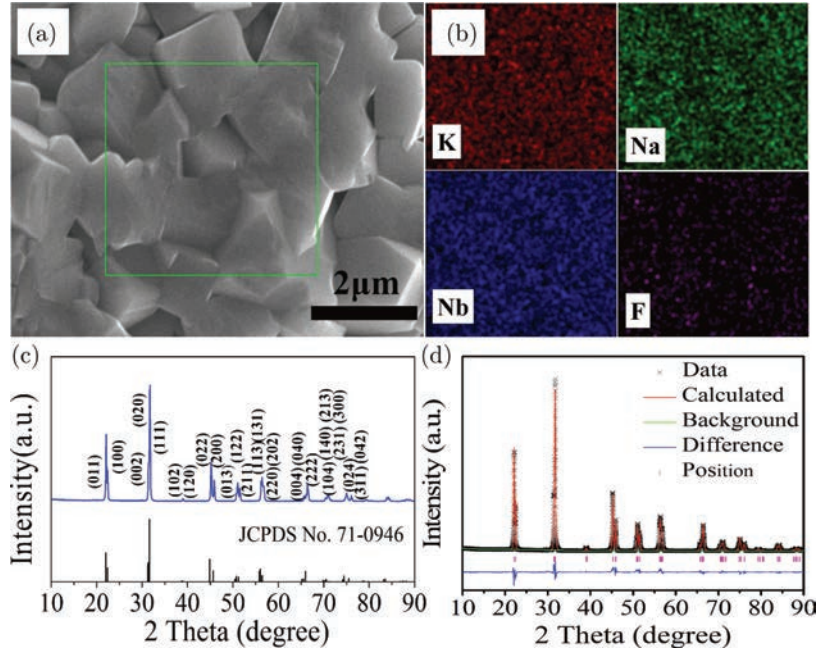


Fig. 1. SEM image of the fracture surface of the low  $pO_2$  fired KNN-LiF ceramic (a); EDS maps of the ceramic (b); XRD curve of the ceramic and JCPDS No. 71-0946 (c); refinement result of the ceramic (d).

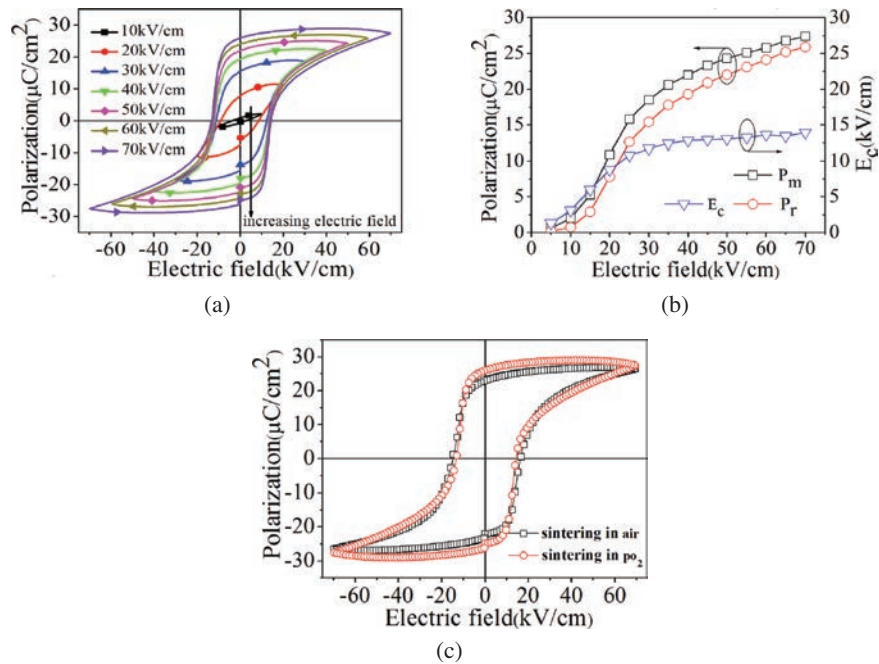


Fig. 2.  $P$ - $E$  loops of the KNN-LiF ceramics sintered in the low  $pO_2$  atmosphere measured at 1 Hz and room temperature under the electric fields from 5 kV/cm to 70 kV/cm (a); the corresponding values of  $E_c$ ,  $P_r$ , and  $P_m$  under various electric fields (b);  $P$ - $E$  loops of the KNN-LiF ceramics sintered in air and  $pO_2$  atmospheres measured at room temperature and 1 Hz under 70 kV/cm (c).

measurement electric field increases, the values of  $P_r$ ,  $P_m$ , and  $E_c$  increase. For the measurement electric field  $E < 25$  kV/cm, the values of  $P_r$ ,  $P_m$ , and  $E_c$  increase rapidly with the increase of the applied electric field. In the case of  $E > 25$  kV/cm, the

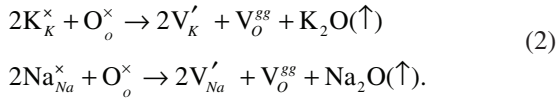
increase of the  $P_r$ ,  $P_m$ , and  $E_c$  values becomes gentle. The  $P$ - $E$  loop of the low  $pO_2$  fired ceramic measured under  $E = 70$  kV/cm is compared with that of the ceramic fired in air [Fig. 2(c)]. At the electric field of  $E = 70$  kV/cm, the values



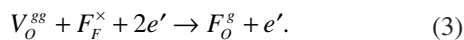
of  $P_m$ ,  $P_r$ , and  $E_c$  of the low pO<sub>2</sub> fired KNN-LiF ceramic are 27.4  $\mu\text{C}/\text{cm}^2$ , 25.9  $\mu\text{C}/\text{cm}^2$ , and 13.9 kV/cm, respectively. The corresponding values of the air fired KNN-LiF ceramic are 26.5  $\mu\text{C}/\text{cm}^2$ , 23  $\mu\text{C}/\text{cm}^2$ , and 15.6 kV/cm, respectively. Compared to the ceramics sintered in air, the low pO<sub>2</sub> sintered ceramics exhibit improved ferroelectric properties, i.e., increased polarization values and decreased coercive field. In addition, the internal bias electric field ( $E_i$ ) was calculated via the following formula:

$$E_i = |E_{c+}| - |E_{c-}|, \quad (1)$$

where  $E_{c+}$  and  $E_{c-}$  represent the positive and negative values of the applied electric field when the polarization intensity is zero, respectively. The  $E_i$  value of the ceramics fired in low pO<sub>2</sub> atmosphere (1.4 kV/cm) is lower than that of the ceramics sintered in air (1.7 kV/cm). The  $E_i$  is closely related to point defects in the ceramics and high  $E_i$  values always correspond to more point defects in the ceramics.<sup>26,27</sup> As is known, K<sup>+</sup> and Na<sup>+</sup> would volatilize during the high-temperature firing process and thus induce cation vacancies and oxygen vacancies in the ceramics, as shown via the Kröger–Vink equation:



The first-principle theoretical analysis has indicated that the activation energy for volatilization of alkali cations increases under sintering in a reducing atmosphere.<sup>28</sup> Therefore, firing in reducing atmosphere is beneficial to suppress the volatilization of cations and reduce cation vacancy concentration. Our previous research on pure K<sub>0.5</sub>Na<sub>0.5</sub>NbO<sub>3</sub> ceramics sintered in the low pO<sub>2</sub> atmosphere shows that the low pO<sub>2</sub> sintering can reduce the weight loss of the sample during sintering.<sup>19</sup> So, it is reasonable to expect that the concentration of point defects in KNN-LiF fired in low pO<sub>2</sub> is decreased compared to that in KNN-LiF sintered in air. As demonstrated above (Fig. 1), Li<sup>+</sup> and F<sup>-</sup> ions have entered into the crystallite lattice and the elements distribute homogeneously. The Li<sup>+</sup> ions will enter into the A-sites due to the similar ion radius with those of K<sup>+</sup> and Na<sup>+</sup>. The substitution of Li<sup>+</sup> for K<sup>+</sup> and Na<sup>+</sup> cannot create charged point defects because of the same electric charge. The radius of F<sup>-</sup> with the coordination number CN = 6 is 1.33 Å, which is similar with that of O<sup>2-</sup>. The F<sup>-</sup> ions can compensate for oxygen vacancies and further reduce amounts of oxygen vacancies and electron defects, as shown in Eq. (3):



The KNN-LiF ceramics sintered in air show electrical resistivity  $\sim 5.2 \times 10^{10} \Omega \cdot \text{cm}$ , while the low pO<sub>2</sub> fired KNN-LiF ceramics exhibit increased electrical resistivity  $\sim 3.2 \times 10^{11} \Omega \cdot \text{cm}$ . The increased resistivity for the low pO<sub>2</sub> fired ceramics demonstrates a decrease in content of point

defects in the ceramics, which facilitates improving ferroelectric properties.

The bipolar strain curves measured at various electric fields ( $E$ ) are demonstrated in Fig. 3(a). The bipolar strain curves demonstrate typical butterfly-like shape. The corresponding maximum positive strain ( $S_{\text{pos}}$ ) and maximum negative strain ( $S_{\text{neg}}$ ) under various measurement electric fields were obtained via the bipolar strain curves and are plotted in Fig. 3(b). The method for calculating  $S_{\text{pos}}$  and  $S_{\text{neg}}$  is also shown in the inset of Fig. 3(b). As the measurement electric fields increase, the absolute values of  $S_{\text{pos}}$  and  $S_{\text{neg}}$  increase gradually. At 65 kV/cm, the values of  $S_{\text{pos}}$  and  $S_{\text{neg}}$  are 0.092% and  $-0.027\%$ , respectively. The unipolar strain curves of the low pO<sub>2</sub> fired KNN-LiF ceramics are shown in Fig. 3(c). As the electric field increases, the unipolar strain values increase gradually. At 65 kV/cm, the maximum strain value ( $S_{\text{max}}$ ) is 0.121%. For comparison, the unipolar strain curves measured at 65 kV/cm for the low pO<sub>2</sub> fired and air fired KNN-LiF ceramics are shown in Fig. 3(d). The air sintered KNN-LiF sample shows the  $S_{\text{max}}$  value only 0.105%, which is lower than that of the low pO<sub>2</sub> fired sample. The low pO<sub>2</sub> fired ceramic exhibits more excellent strain performance. The inverse piezoelectric constant  $d_{33}^*$  is calculated via Eq. (4):

$$d_{33}^* = S_{\text{max}}/E_{\text{max}}, \quad (4)$$

where  $E_{\text{max}}$  is the maximum electric field. The  $d_{33}^*$  values of the ceramics fired in the low pO<sub>2</sub> and air atmospheres are 186 pm/V and 161 pm/V, respectively. As the KNN-LiF samples were fired in the low pO<sub>2</sub> atmosphere, they exhibit higher  $d_{33}^*$ . The ceramics sintered in low pO<sub>2</sub> and air atmospheres exhibit the  $d_{33}$  values of 125 pC/N and 114 pC/N, respectively. The pure KNN ceramics with adding some simple oxides or fluorides sintered in air always exhibit relatively low  $d_{33}$  values. For examples, it has been reported that the ceramics KNN-1.5mol% CuF<sub>2</sub>,<sup>29</sup> KNN-0.5mol% MnO<sub>2</sub>,<sup>30</sup> KNN-ZrO<sub>2</sub>,<sup>31</sup> KNN-0.4wt% CuO,<sup>32</sup> KNN-1mol% SnO<sub>2</sub>,<sup>33</sup> and KNN-KF<sup>9</sup> have  $d_{33}$  values of 96 pC/N, 111 pC/N, 100 pC/N, 55 pC/N, 108 pC/N, and 105 pC/N, respectively. In this work, the ceramic KNN-LiF sintered in air shows  $d_{33}$  of 114 pC/N. If the low pO<sub>2</sub> firing atmosphere was used, the  $d_{33}$  of KNN-LiF can be further increased to 125 pC/N. The low pO<sub>2</sub> fired KNN-LiF ceramics exhibit higher  $d_{33}$ . Piezoelectric constant  $d_{33}$  is related to polarization, as shown in Eq. (5):

$$d_{33} \approx \epsilon_{33}\epsilon_0QP_r, \quad (5)$$

in which  $\epsilon_{33}$  is intrinsic dielectric constant,  $\epsilon_0$  is the vacuum dielectric constant,  $Q$  is the electrostriction coefficient, and  $P_r$  is the remnant polarization.<sup>34</sup> Excellent ferroelectric properties with high polarization of the low pO<sub>2</sub> fired KNN-LiF ceramics correspond to high  $d_{33}$  of the ceramics.

Dielectric constant ( $\epsilon_r$ ) and dielectric loss ( $\tan\delta$ ) of the low pO<sub>2</sub> fired ceramic as a function of measurement temperature ( $T$ ) are demonstrated in Fig. 4. The dielectric spectra are similar with those of the other fluorides-added KNN-based ceramics.<sup>9,17</sup> Two dielectric peaks appear on the  $\epsilon_r$ - $T$  curves,

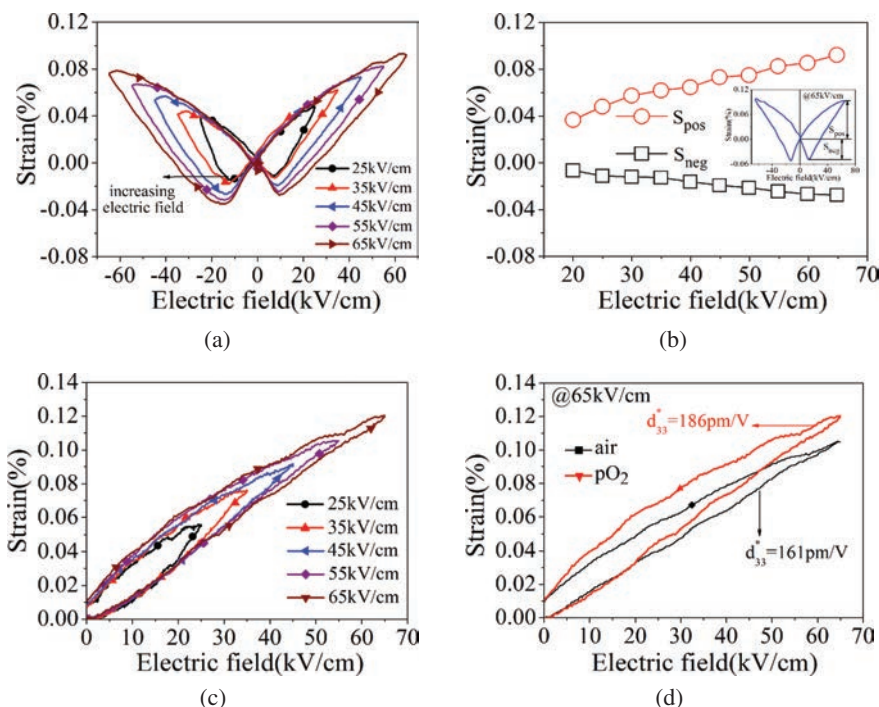


Fig. 3. Bipolar strain curves of the KNN-LiF ceramics sintered in the low pO<sub>2</sub> atmosphere measured at room temperature and 1 Hz under various electric fields (a); the corresponding values of S<sub>pos</sub> and S<sub>neg</sub> (b). The inset in (b) shows the method to calculate S<sub>pos</sub> and S<sub>neg</sub>. Unipolar strain curves of the KNN-LiF ceramics sintered in the low pO<sub>2</sub> atmosphere measured at room temperature and 1 Hz under various electric fields (c); Unipolar strain curves of the KNN-LiF ceramics sintered in the low pO<sub>2</sub> and air atmospheres measured at 65 kV/cm (d).

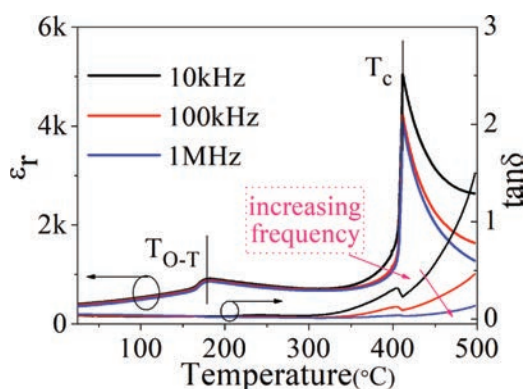


Fig. 4. Dielectric constant ( $\epsilon_r$ ) and dielectric loss ( $\tan\delta$ ) of the KNN-LiF ceramics sintered in the low pO<sub>2</sub> atmosphere versus temperature.

corresponding to the phase transition between the orthorhombic phase and tetragonal phase around the temperature  $T_{O-T}$  and that from the tetragonal phase to the cubic phase around the temperature  $T_c$ . Both the phase transition temperatures do not change with changing the measurement frequencies. The values of  $T_{O-T}$  and  $T_c$  are 177 °C and 410 °C, respectively. The values of  $\tan\delta$  and  $\epsilon_r$  at room temperature are 0.03 and 451, respectively. For the low pO<sub>2</sub> fired pure KNN ceramics,<sup>19</sup> the values of  $T_{O-T}$ ,  $T_c$ ,  $\tan\delta$ , and  $\epsilon_r$  are 195 °C, 406 °C, 0.04,

and 366, respectively. The LiF-added KNN ceramics sintered in the low pO<sub>2</sub> atmosphere exhibit increased  $\epsilon_r$  and  $T_c$ , decreased  $\tan\delta$  and  $T_{O-T}$  compared to the low pO<sub>2</sub> fired pure KNN ceramics. In our previous work, the pure K<sub>0.5</sub>Na<sub>0.5</sub>NbO<sub>3</sub> ceramics without any dopant were also sintered in air<sup>12</sup> and low oxygen partial pressure atmosphere.<sup>19</sup> The ferroelectric and piezoelectric properties of the pure K<sub>0.5</sub>Na<sub>0.5</sub>NbO<sub>3</sub> and KNN-LiF sintered in different atmospheres are compared in Table 1. The phase transition temperatures can affect piezoelectric properties of the ceramics. It has been widely reported that the piezoelectric constant  $d_{33}$  can be greatly improved by decreasing the phase transition temperature  $T_{O-T}$  towards to room temperature.<sup>3,6</sup> Here, the LiF-added KNN ceramic sintered in the low pO<sub>2</sub> atmosphere shows lower  $T_{O-T}$  (177 °C) and higher  $d_{33}$  (125 pC/N) compared to the low pO<sub>2</sub> fired pure KNN ceramic ( $T_{O-T}$  = 195 °C,  $d_{33}$  = 112 pC/N).<sup>19</sup> Compared to the KNN-LiF ceramic sintered in air ( $T_{O-T}$  = 178 °C,  $d_{33}$  = 114 pC/N), the KNN-LiF ceramic sintered in the low pO<sub>2</sub> atmosphere exhibits decreased  $T_{O-T}$  and increased  $d_{33}$  (Table 1). Compared to the pure KNN ceramic sintered in the low pO<sub>2</sub> ( $T_{O-T}$  = 195 °C,  $d_{33}$  = 112 pC/N), the pure KNN ceramic sintered in air shows decreased  $T_{O-T}$  (191 °C) and decreased  $d_{33}$  (60 pC/N), which is mainly due to its lower density (88%) (Table 1). From Table 1, it is found that the present low pO<sub>2</sub> fired KNN-LiF ceramics exhibit the highest  $\rho_r$ ,  $d_{33}$ ,  $d_{33}^*$ ,  $P_r$  values, and the lowest  $\tan\delta$ ,  $E_p$ ,  $E_c$  values. The

Table 1. Comparison of ferroelectric and piezoelectric properties of the  $K_{0.5}Na_{0.5}NbO_3$  (KNN) and KNN-LiF ceramics sintered in different atmospheres.

Samples	KNN	KNN	KNN-LiF	KNN-LiF
pO <sub>2</sub> value	Air	10 <sup>-6</sup> atm	Air	10 <sup>-12</sup> atm
$\rho_r$ (%)	88%	95%	92%	>96%
tan $\delta$ (1 kHz)	0.46	0.04	0.04	0.03
$\epsilon_r$ (1 kHz)	183	366	474	451
$d_{33}$ (pC/N)	60	112	114	125
$d_{33}^*$ (pm/V)	—	119	161	186
$P_r$ ( $\mu$ C/cm <sup>2</sup> )	6.5	21.6	23.0	25.9
$E_c$ (kV/cm)	17.5	15.5	15.6	13.9
$E_i$ (kV/cm)	—	2.7	1.7	1.4
$T_{O-T}$ (°C)	191	195	178	177
$T_c$ (°C)	400	406	415	410
$Q_m$	—	143	94	125
$k_p$	—	0.29	0.29	0.26
Resistivity ( $\Omega \cdot$ cm)	$\sim 10^8$	—	$5.2 \times 10^{10}$	$3.2 \times 10^{11}$
Ref.	12	19	this work	this work

result show that the low pO<sub>2</sub> sintering and addition of LiF are efficient in improving electrical properties of KNN ceramics with the simple composition.

In order to detect whether the present pO<sub>2</sub> value is low enough so that the base metals such as Ni and Cu cannot be oxidized, the metal powders of 10 wt.% Cu and 10 wt.% Ni were separately mixed into the KNN-LiF precursor powders and co-fired at 1065 °C for 3 h in the low pO<sub>2</sub> atmosphere. The obtained samples were denoted as KNN-LiF+Cu and KNN-LiF+Ni, respectively. The XRD curves of the obtained samples are exhibited in Fig. 5. For comparison, the XRD curves of the Cu and Ni raw powders were also measured. For both the KNN-LiF+Cu and KNN-LiF+Ni samples, there exist only two phases, i.e., the perovskite structure and Cu or Ni phase. No other phases such as oxides of Cu/Ni or chemical reaction products between Cu/Ni and KNN-LiF were observed. In the present low pO<sub>2</sub> atmosphere, the base metals including Cu and Ni cannot be oxidized, suggesting a possible route to use base metals as electrodes.

#### 4. Conclusions

Compared to the  $(Na_{0.5}K_{0.5})NbO_3$ -2mol% LiF ceramics fired in air and pure  $(Na_{0.5}K_{0.5})NbO_3$  ceramics fired in low pO<sub>2</sub> atmosphere, the  $(Na_{0.5}K_{0.5})NbO_3$ -2mol% LiF ceramics fired in the low pO<sub>2</sub> atmosphere show improved ferroelectric and piezoelectric properties. The present samples exhibit  $d_{33}$  of 125 pC/N,  $d_{33}^*$  of 186 pm/V,  $\epsilon_r$  of 451, tan $\delta$  of 0.03,  $T_{O-T}$  of 177 °C,  $T_c$  of 410 °C,  $P_m$  of 27.4  $\mu$ C/cm<sup>2</sup>,  $P_r$  of 25.9  $\mu$ C/cm<sup>2</sup>,  $E_c$  of 13.9 kV/cm,  $S_{pos}$  of 0.092%, and  $S_{neg}$  of -0.027%.

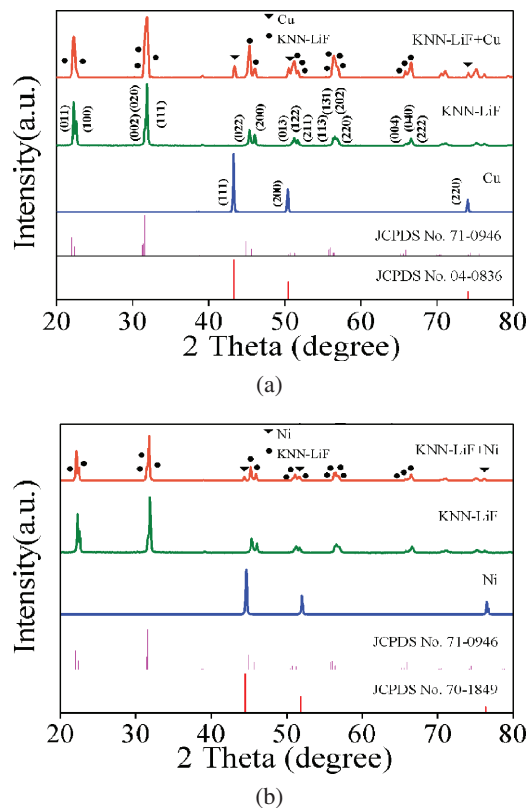


Fig. 5. XRD curves of KNN-LiF+Cu sintered in the low pO<sub>2</sub> atmosphere and raw powder of Cu (a). XRD curves of KNN-LiF+Ni sintered in the low pO<sub>2</sub> atmosphere and raw powder of Ni (b). For comparison, the XRD curve of the KNN-LiF ceramic sintered in the low pO<sub>2</sub> atmosphere are also shown in (a) and (b). In the bottom of the figures, the corresponding JCPDS Nos. are shown.

The base metals such as Cu and Ni inside the ceramics cannot be oxidized after firing in the low pO<sub>2</sub> atmosphere, implying a possible route to use base metals as electrodes.

#### Acknowledgments

This work was supported by National Natural Science Foundation of China (No. 51972202), Fundamental Research Funds for the Central Universities (No. GK201901005, 2019CSLY006).

#### References

- H. Tao, H. Wu, Y. Liu, Y. Zhang, J. Wu, F. Li, X. Lyu, C. Zhao, D. Xiao, J. Zhu and S. J. Pennycook, Ultrahigh performance in lead-free piezoceramics utilizing a relaxor slush polar state with multiphase coexistence, *J. Am. Chem. Soc.* **141**, 13987 (2019).
- B. Wu, J. Ma, Q. Gou, W. Wu and M. Chen, Enhanced temperature stability in the O-T phase boundary of (K,Na)NbO<sub>3</sub>-based ceramics, *J. Am. Ceram. Soc.* **103**, 1698 (2019).
- A. Khesro, D. Wang, F. Hussain, R. Muhammad, G. Wang, A. Feteira and I. M. Reaney, Temperature dependent piezoelectric properties of lead-free  $(1-x)K_{0.6}Na_{0.4}NbO_3-xBiFeO_3$  ceramics, *Front. Mater.* **7**, 140 (2020).



- <sup>4</sup>D. Wang, F. Hussain, A. Khesro, A. Feteira, Y. Tian, Q. Zhao and I. M. Reaney, Composition and temperature dependence of structure and piezoelectricity in  $(1-x)(K_{1-x}Na_x)NbO_3-x(Bi_{1/2}Na_{1/2})ZrO_3$  lead-free ceramics, *J. Am. Ceram. Soc.* **100**, 627 (2017).
- <sup>5</sup>T. Zheng, J. Wu, D. Xiao and J. Zhu, Giant  $d_{33}$  in nonstoichiometric  $(K,Na)NbO_3$ -based lead-free ceramics, *Scr. Mater.* **94**, 25 (2015).
- <sup>6</sup>J. Wu, D. Xiao and J. Zhu, Potassium-sodium niobate lead-free piezoelectric materials: Past, present, and future of phase boundaries, *Chem. Rev.* **115**, 2559 (2015).
- <sup>7</sup>C. Liu, P. Liu, K. Kobayashi, W. G. Qu and C. A. Randall, Enhancement of piezoelectric performance of lead-free NKN-based ceramics via a high-performance flux- $NaF-Nb_2O_5$ , *J. Am. Ceram. Soc.* **96**, 3120 (2013).
- <sup>8</sup>X. Lv, J. Wu and X.-X. Zhang, Reduced degree of phase coexistence in KNN-based ceramics by competing additives, *J. Eur. Ceram. Soc.* **40**, 2945 (2020).
- <sup>9</sup>H. S. Huang, X. M. Chen, J. B. Lu and H. L. Lian, Ferroelectric and dielectric properties of KF-added  $(K_{0.48}Na_{0.52})NbO_3$  lead-free ceramics, *Phys. B: Condens. Matter.* **564**, 28 (2019).
- <sup>10</sup>Z. Shen, D. Grüner, M. Eriksson, L. M. Belova, C.-W. Nan and H. Yan, Ordered coalescence of nano-crystals in alkaline niobate ceramics with high remanent polarization, *J. Materiomics* **3**, 267 (2017).
- <sup>11</sup>G. Ye, J. Wade-Zhu, J. Zou, T. Zhang, T. W. Button and J. Binner, Microstructures, piezoelectric properties and energy harvesting performance of undoped  $(K_{0.5}Na_{0.5})NbO_3$  lead-free ceramics fabricated via two-step sintering, *J. Eur. Ceram. Soc.* **40**, 2977 (2020).
- <sup>12</sup>Y. L. Su, X. M. Chen, Z. D. Yu, H. L. Lian, D. D. Zheng and J. H. Peng, Comparative study on microstructure and electrical properties of  $(K_{0.5}Na_{0.5})NbO_3$  lead-free ceramics prepared via two different sintering methods, *J. Mater. Sci.* **52**, 2934 (2017).
- <sup>13</sup>Z. D. Yu, X. M. Chen, Y. L. Su, H. L. Lian, J. B. Lu, J. P. Zhou and P. Liu, Hot-press sintering  $K_{0.5}Na_{0.5}NbO_3-0.5mol\%Al_2O_3$  ceramics with enhanced ferroelectric and piezoelectric properties, *J. Mater. Sci.* **54**, 13457 (2019).
- <sup>14</sup>T. Reimann, S. Fröhlich, A. Bochmann, A. Kynast, M. Töpfer, E. Hennig and J. Töpfer, Low  $pO_2$  sintering and reoxidation of lead-free KNNLT piezoceramic laminates, *J. Eur. Ceram. Soc.* **41**, 344 (2021).
- <sup>15</sup>B. Malič, J. Koruza, J. Hreščak, J. Bernard, K. Wang, J. Fisher and A. Benčan, Sintering of lead-free piezoelectric sodium potassium niobate ceramics, *Mater.* **8**, 8117 (2015).
- <sup>16</sup>J. G. Fisher, D. Rout, K.-S. Moon and S.-J. L. Kang, High-temperature X-ray diffraction and Raman spectroscopy study of  $(K_{0.5}Na_{0.5})NbO_3$  ceramics sintered in oxidizing and reducing atmospheres, *Mater. Chem. Phys.* **120**, 263 (2010).
- <sup>17</sup>K. Kobayashi, Y. Doshida, Y. Mizuno, C. A. Randall and D. Damjanovic, A route forwards to narrow the performance gap between PZT and lead-free piezoelectric ceramic with low oxygen partial pressure processed  $(Na_{0.5}K_{0.5})NbO_3$ , *J. Am. Ceram. Soc.* **95**, 2928 (2012).
- <sup>18</sup>Z. Cen, X. Wang, Y. Huan, Y. Zhen, W. Feng and L. Li, Defect engineering on phase structure and temperature stability of KNN-based ceramics sintered in different atmospheres, *J. Am. Ceram. Soc.* **101**, 3032 (2018).
- <sup>19</sup>Z. D. Yu, X. M. Chen, H. L. Lian, Q. Zhang and W. X. Wu, Microstructure and electrical properties of  $K_{0.5}Na_{0.5}NbO_3$  lead-free piezoelectric ceramics sintered in low  $pO_2$  atmosphere, *J. Mater. Sci.: Mater. Electron.* **29**, 19043 (2018).
- <sup>20</sup>R. Marder, R. Chaim, G. Chevallier and C. Estournès, Effect of 1wt% LiF additive on the densification of nanocrystalline  $Y_2O_3$  ceramics by spark plasma sintering, *J. Eur. Ceram. Soc.* **31**, 1057 (2011).
- <sup>21</sup>R. D. Shannon, Revised effective ionic radii and systematic studies of interatomic distances in halides and chalcogenides, *Acta Cryst. Sec. A* **32**, 751 (1976).
- <sup>22</sup>D. Wang, Z. Fan, W. Li, D. Zhou, A. Feteira, G. Wang, S. Murakami, S. Sun, Q. Zhao, X. Tan and I. M. Reaney, High energy storage density and large strain in  $Bi(Zn_{2/3}Nb_{1/3})O_3$ -doped  $BiFeO_3-BaTiO_3$  ceramics, *ACS Appl. Energy Mater.* **1**, 4403 (2018).
- <sup>23</sup>L.-N. Liu, X.-M. Chen, R.-Y. Jing, H.-L. Lian, W.-W. Wu, Y.-P. Mou and P. Liu, Electrical and photoluminescence properties of  $(Bi_{0.5-x/0.94}Er_{x/0.94}Na_{0.5})_{0.94}Ba_{0.06}TiO_3$  lead-free ceramics, *J. Mater. Sci.: Mater. Electron.* **30**, 5233 (2019).
- <sup>24</sup>J. G. Fisher, A. Benčan, J. Bernard, J. Holc, M. Kosec, S. Vernay and D. Rytz, Growth of  $(Na,K,Li)(Nb, Ta)O_3$  single crystals by solid state crystal growth, *J. Eur. Ceram. Soc.* **27**, 4103 (2007).
- <sup>25</sup>JCPDS-ICDD Card, International centre for diffraction data, (Newtown Square, PA, 2002).
- <sup>26</sup>L. Enzhu, H. Kakemoto, S. Wada and T. Tsurumi, Enhancement of  $Q_m$  by co-doping of Li and Cu to potassium sodium niobate lead-free ceramics, *IEEE Trans. Ultrason. Ferroelectr. Freq. Control* **55**, 980 (2008).
- <sup>27</sup>X.-S. Qiao, X.-M. Chen, H.-L. Lian, W.-T. Chen, J.-P. Zhou, P. Liu and S. Zhang, Microstructure and electrical properties of nonstoichiometric  $0.94(Na_{0.5}Bi_{0.5+x})TiO_3-0.06BaTiO_3$  lead-free ceramics, *J. Am. Ceram. Soc.* **99**, 198 (2016).
- <sup>28</sup>J. D. T. Richard, *Defect in Solids* (John Wiley & Sons, 2008.)
- <sup>29</sup>C.-M. Weng, C.-C. Tsai, J. Sheen, C.-S. Hong, S.-Y. Chu, Z.-Y. Chen and H.-H. Su, Low-temperature-sintered  $CuF_2$ -doped NKN ceramics with excellent piezoelectric and dielectric properties, *J. Alloys Compd.* **698**, 1028 (2017).
- <sup>30</sup>D. Lin, Q. Zheng, K. W. Kwok, C. Xu and C. Yang, Dielectric and piezoelectric properties of  $MnO_2$ -doped  $K_{0.5}Na_{0.5}Nb_{0.92}Sb_{0.08}O_3$  lead-free ceramics, *J. Mater. Sci. Mater. Electron.* **21**, 649 (2009).
- <sup>31</sup>B. Malic, J. Bernard, A. Bencan and M. Kosec, Influence of zirconia addition on the microstructure of  $K_{0.5}Na_{0.5}NbO_3$  ceramics, *J. Eur. Ceram. Soc.* **28**, 1191 (2008).
- <sup>32</sup>K. Chen, J. Zhou, F. Zhang, X. Zhang, C. Li, L. An and J. R. G. Evans, Screening sintering aids for  $(K_{0.5}Na_{0.5})NbO_3$  ceramics, *J. Am. Ceram. Soc.* **98**, 1698 (2015).
- <sup>33</sup>R. Zuo, J. Rodel, R. Chen and L. Li, Sintering and electrical properties of lead-free  $Na_{0.5}K_{0.5}NbO_3$  piezoelectric ceramics, *J. Am. Ceram. Soc.* **89**, 2010 (2006).
- <sup>34</sup>A. Safari and E. K. Akdoğan, *Piezoelectric and Acoustic Materials for Transducer Applications* (Springer, New York, N.J. 2008), p. 21.